SUPPLEMENTARY INFORMATION

S1. FTIR and DSC analyses:

Characteristic peaks of ASPM (1703.14 cm^{-1}, 1612.49 cm^{-1} (aryl C=C), 1570.06 cm^{-1} (aryl =C-H) and 1481.33 cm^{-1} (aryl =C-H)) were observed in the FTIR spectrum of physical mixture of ASPM, DSPC and cholesterol. The comparison between FTIR spectrum of placebo liposomes and ASPM liposomes showed the presence of specific functional groups of excipients in ASPM liposomes same as those in placebo liposomes (Figure S1). DSC thermogram revealed that ASPM presented the corresponding endothermic peak at 146.62 ºC. The melting point of cholesterol appeared at 149.52 ºC, which found to be decreased in placebo liposomes may be due to moistening effect of DSPC (Victoria and David, 2003). Similarly, DSC thermogram of ASPM liposomes showed DSPC peak at 50.94 ºC. This DSC thermogram showed two minor peaks, although there was a broad peak by joining these two peaks; one at 122.49 ºC and the other one at 131.76 ºC. Hence based on cholesterol peaks in its plain form as well as in placebo, the peak 122.49 ºC may correspond to cholesterol and the other one at 131.76 ºC may correspond to ASPM. The decrease in ASPM melting endotherm may be due to the partial amorphization of the drug in liposomal form. At the same time, there was a broad peak formed with an Onset and Endset of 114.68 ºC and 144.16 ºC and the peak value was 131.76 ºC. This broad peak at the melting range of ASPM indicates the loss of crystallinity of drug, which might have molecularly dispersed in the lipid matrix (Shete and Patravale, 2013). The comparison of all DSC thermograms does not reveal any chemical incompatibility between ASPM and excipients and shows the amorphization of the drug in the liposomal form.

S2. Lipid recovery quantification

Stewart's reagent, 0.1 M ammonium ferrothiocyanate, was prepared by dissolving 5.46 g ferric chloride hexahydrate and 6.08 g ammonium thiocyanate in 200 mL of deionized water. To 50 µL of the lipid sample, 2 mL of chloroform and 2 mL of Stewart's reagent was incorporated, and the mixture was centrifuged at 1000 g for 10 min. The lower organic layer was removed and analyzed by UV-Vis spectrophotometer at 470 nm. A calibration curve was prepared in the same way using known amounts of lipid as standards and the lipid recovery was determined by comparing the lipid concentration before and after size exclusion chromatography.

S3. Preparation of FITC-labelled liposomes

FITC labelled liposomes were prepared according to previously published literature. Briefly, prepared liposomes were incubated with ethanolic solution of FITC (0.5 mg/mL) with continuous stirring. The FITC labelled liposomes were separated by centrifugation (16000 rpm/ 15 min).

S4. Optimization of liposomes formulation

Parameters involved in the preparation of liposomes such as total lipid amount, cholesterol content, drug amount and sonication parameters (amplitude and time) were optimized by varying one-factor at a time. The optimization results of ASPM liposomes are shown in Table S1. An increase in total lipid amount from 1 to 2% w/v was found to decrease the particle size. Liposomes found to be monodispersed with low PDI values. As the total lipid amount increased from 2 to 3% w/v, particle size and PDI increased. The entrapment efficiency of liposomes increased with increase in total lipid amount However, further increase in total lipid amount resulted in decreased entrapment efficiency. Zeta potential shifted towards negative values upon increasing the total lipid amount. As the cholesterol content (molar ratio of DSPC: cholesterol) increased in the liposomes from 1:0.025 to 1:1, particle size, entrapment efficiency and negativity of zeta potential also increased.

When the amount of drug increased from 0.0025% w/w to 0.0075% w/w, particle size also increased. Initially, when drug quantity increased from 0.0025% w/w (LP-8) to 0.005% w/w (LP-3), entrapment efficiency also increased. However, a further increase in drug amount (0.0075% w/w), there was a decrease in entrapment efficiency. Zeta potential shifted to more negative values; but then decreased eventually.

As the sonication time was increased gradually from 5 to 15 min, particle size as well as PDI was decreased. When sonication time was increased from 5 to 10 min, slight increase in entrapment efficiency was observed. Further increase in time from 10 min to 15 min, there was a drastic decrease in the entrapment efficiency. Zeta potential was almost similar upon increasing the sonication time.

As the sonication amplitude increased from 40% to 60%, decrease in particle size and PDI was observed. At 80% amplitude, increase in size and PDI was noticed along with an increase in turbidity of dispersion. Increase in entrapment efficiency was observed upon increasing sonication amplitude from 40% to 60%. However, at 80% amplitude, a drastic decrease in entrapment efficiency was observed. There was no change in zeta potential with the increase in sonication amplitude.

S5. Optimization of Liposomes

Increase in total lipid amount from 1% w/v to 2% w/v was found to decrease the particle size, which may be because of reorganization of lipid bilayer resulting in more number of narrow sized small particles. As the total lipid amount was increased from 2% w/v to 3% w/v, particle size and PDI was increased. This may be because at their high concentrations, lipids merge together thereby increasing the viscosity of the lipid phase, which affects the shearing capacity of probe-sonicator (Martins et al., 2012). This may also be a reason for the considerable increase in PDI on increasing the total lipid amount. When the total lipid amount was increased from 1% w/v to 2% w/v, the entrapment efficiency of liposomes was increased. This may be due to the availability of more space to entrap more drug into the vesicles. However, a further increase in total lipid amount resulted in decreased entrapment efficiency suggesting the coalescence of lipid particles, thereby expelling out some of the entrapped drug. Increased particle size suggests possible merging of lipid vesicles upon increasing the total lipid amount. Liposomes showed negative zeta potential due to the negative charge obtained from phosphate group of DSPC. Zeta potential was shifted more towards negative value upon increasing the total lipid amount because of more number of negative phosphate groups at the liposomal surface.

Cholesterol acts as a lipid bilayer membrane stabilizer and makes the bilayer more rigid and hence this might have resulted in increased particle size. Higher lipophilicity resulted by increased cholesterol content might have increased the entrapment efficiency. When cholesterol content was increased, a slight increase in negativity of zeta potential was observed which may be because of the less availability of adsorbed free drug on the surface of liposomes as a result of increased entrapment capacity of vesicles.

When the amount of drug was increased, particle size was also increased, which could be due to the extra layer of the adsorbed free drug onto the surface of liposomes. Initially, when drug quantity was increased, entrapment efficiency was also increased. However, further increase in drug amount led to decreased entrapment efficiency because of the saturation of entrapping capacity of the vesicles. The initial increase in negative zeta potential was an indication of less free drug at the surface of liposomes (more drug entrapment); but later zeta potential was decreased drastically, which may be because of the presence of more adsorbed free drug at the liposomal surface.

As the sonication time was increased gradually from 5 to 15 min, the particle size was decreased because of ultrasound energy. PDI was also shown to decrease upon increasing the time of sonication as homogeneous particles were obtained after sonication. When sonication

time was increased from 5 to 10 min, a slight increase in entrapment efficiency was observed. Further increase in time from 10 min to 15 min, there was a drastic decrease in the entrapment efficiency. This may be due to a decrease in stability of dispersion with an increase in cavitation energy, leading to agglomeration. Zeta potential was almost similar upon increasing the sonication time.

As the sonication amplitude was increased from 40%, a decrease in particle size and PDI was observed because of effective ultrasound energy. At 80% amplitude, increase in size and PDI was noticed along with an increase in turbidity of dispersion. This may be due to a decrease in stability of dispersion with an increase in cavitation energy thereby leading to agglomeration (Sugita et al., 2013). Increase in entrapment efficiency was observed upon increasing sonication amplitude from 40% to 60%. However, at 80% amplitude, a drastic decrease in entrapment efficiency was observed, which may be due to the instability of liposomes caused by heat generated upon sonication. Zeta potential was found to be unaffected with the increase in sonication amplitude as there is no change in net charge.

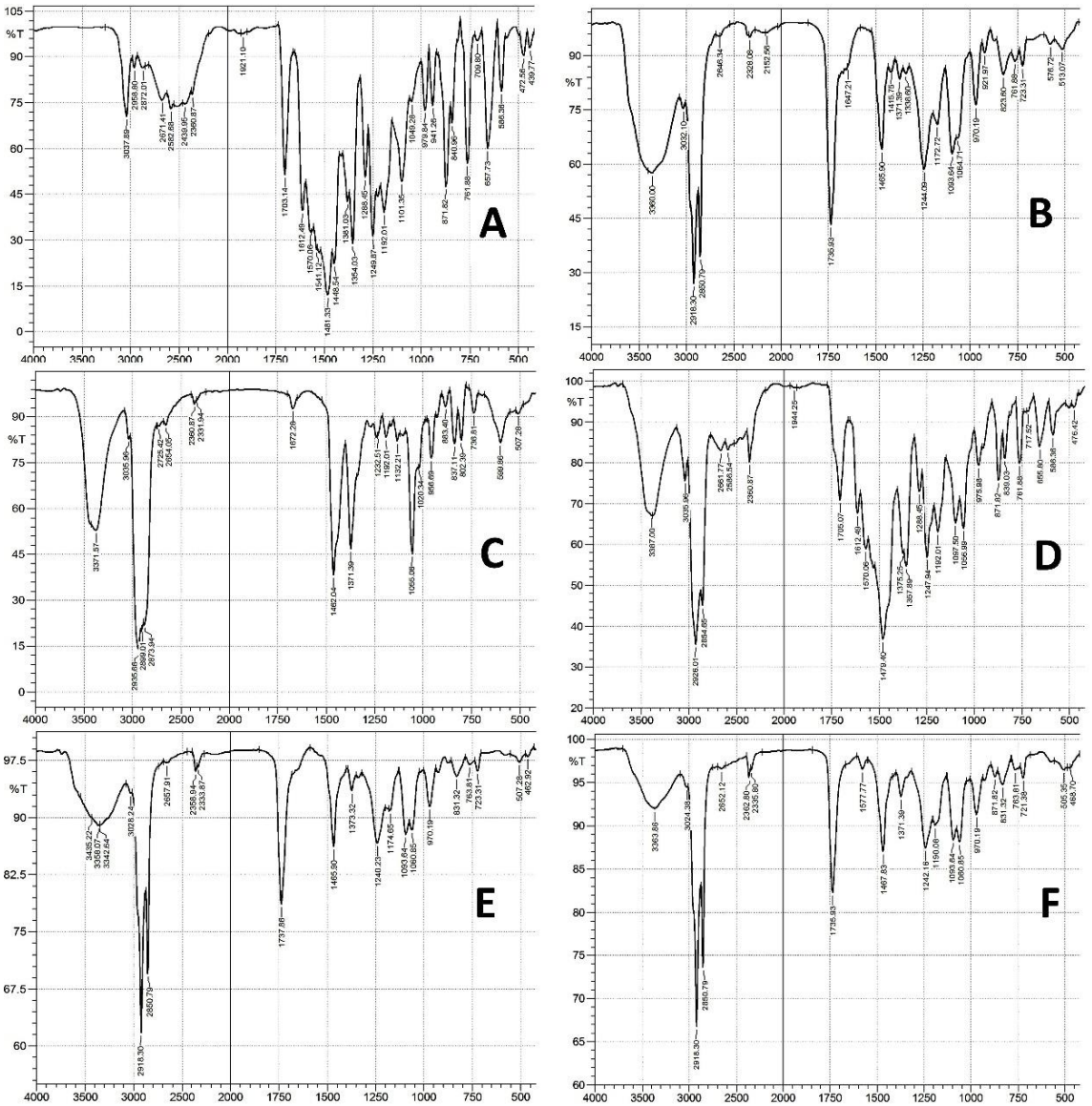

Figure S1. FTIR spectra of (A) ASPM, (B) DSPC, (C) cholesterol, (D) ASPM-DSPC-cholesterol physical mixture, (E) placebo liposomes and (F) ASPM liposomes.

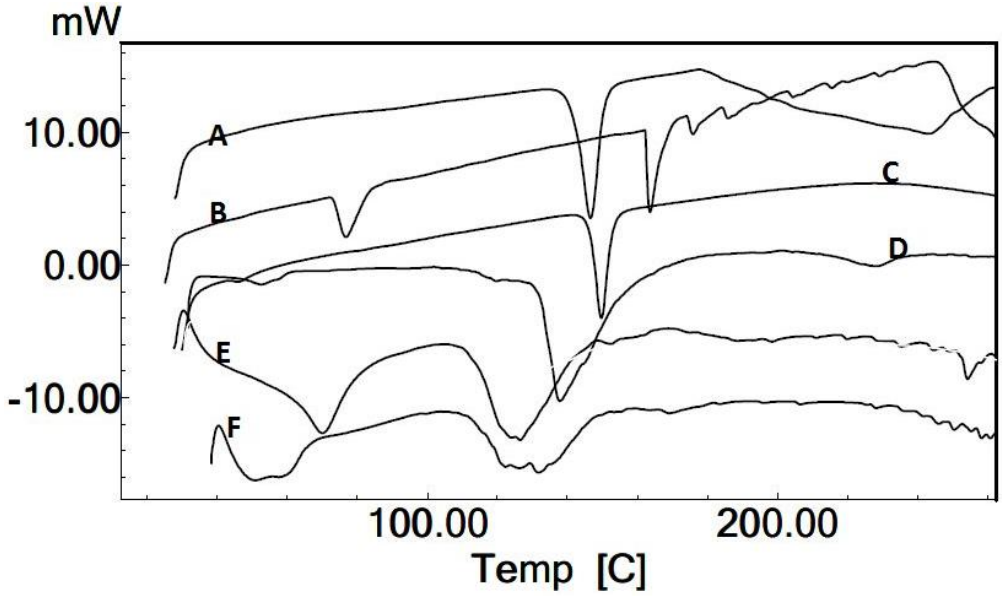

Figure S2. DSC thermograms of (A) ASPM, (B) DSPC, (C) cholesterol, (D) ASPM-DSPC-cholesterol physical mixture, (E) placebo liposomes and (F) ASPM liposomes.

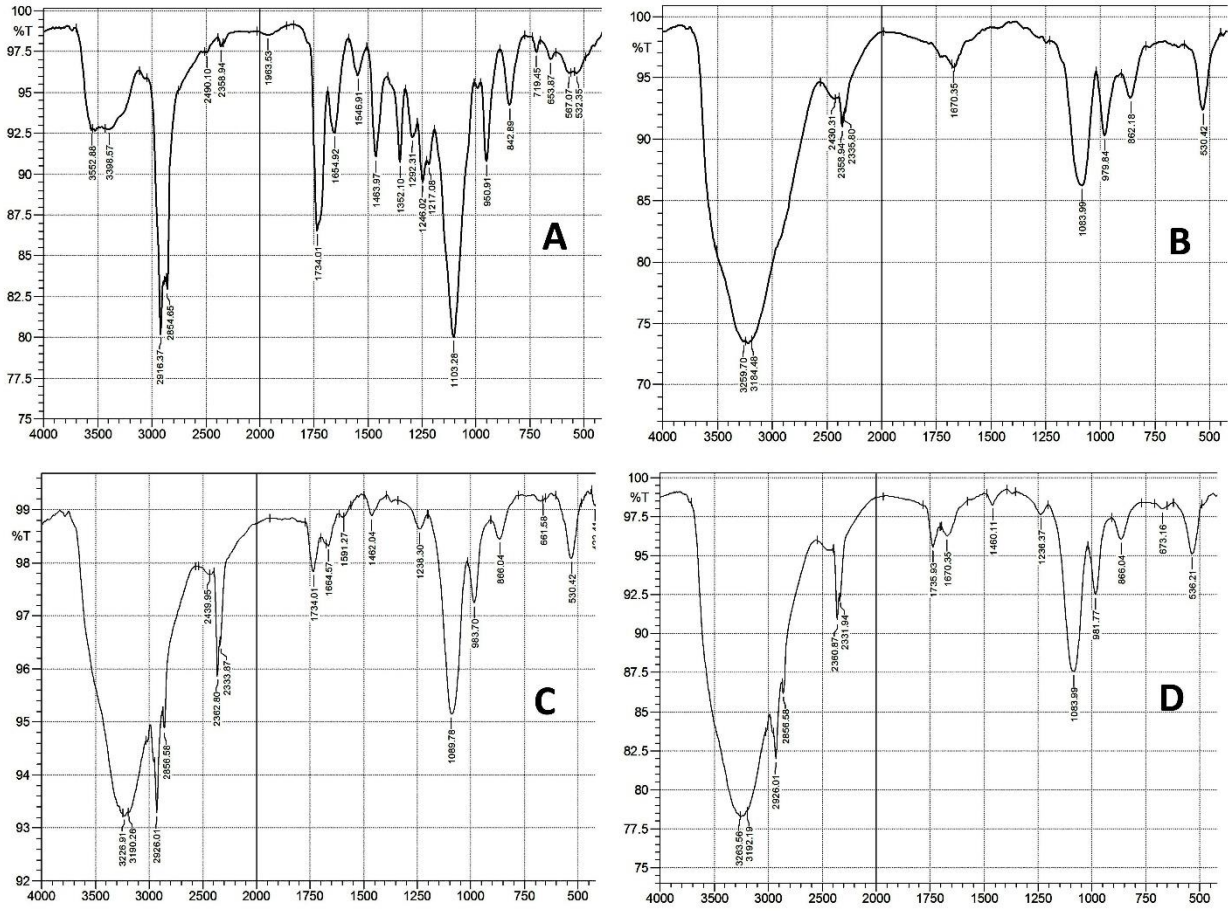

Figure S3. FTIR spectra of (A) DSPE-PEG-COOH, (B) DSPE-PEG-RGD, (C) LP-COOH, (D) LP-CONH-RGD

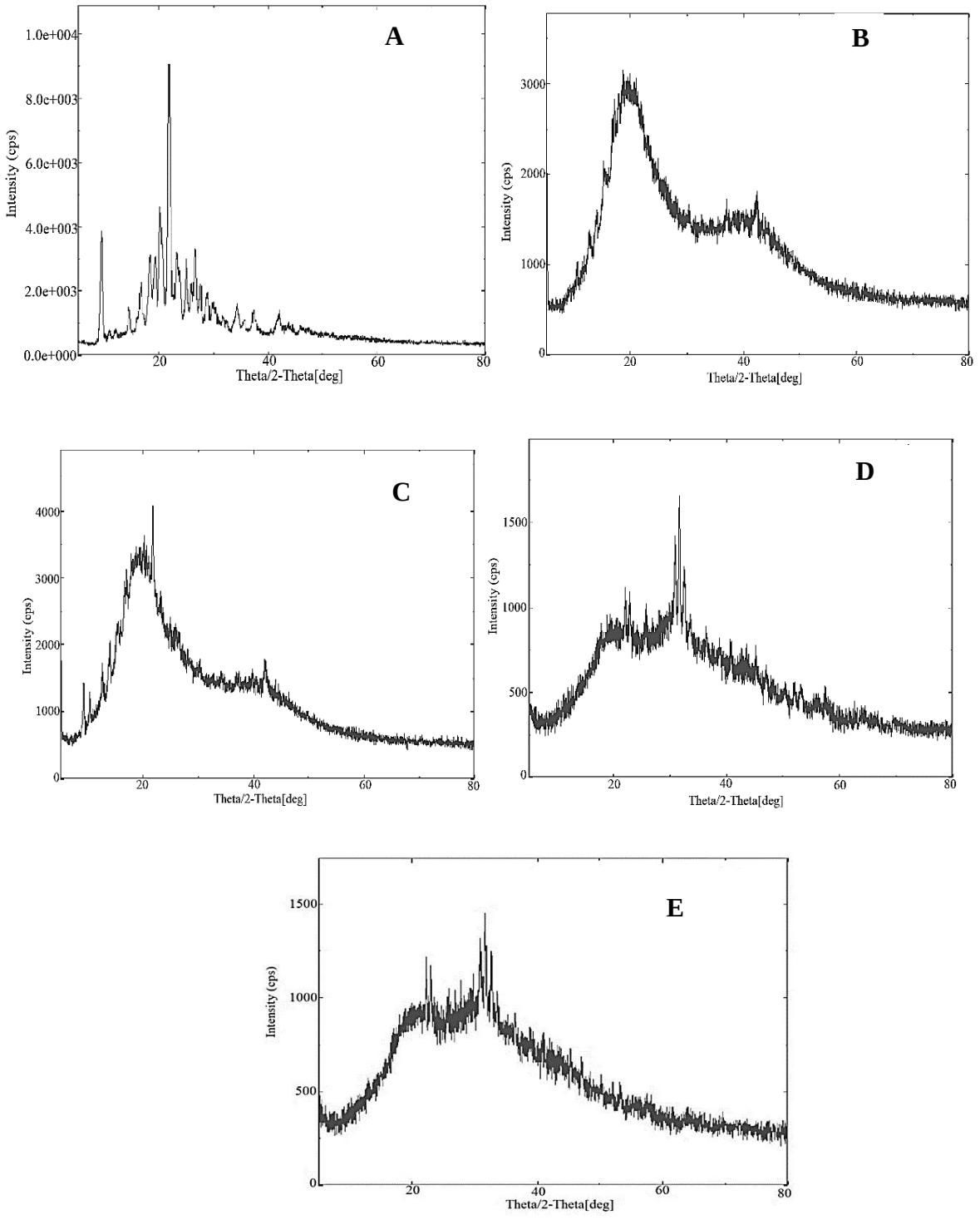

Figure S4. XRD Patterns (A) ASPM, (B) DSPC-CHOL, (C) ASPM-DSPC-CHOL physical mixture, (D) Placebo liposomes and (E) ASPM liposomes.

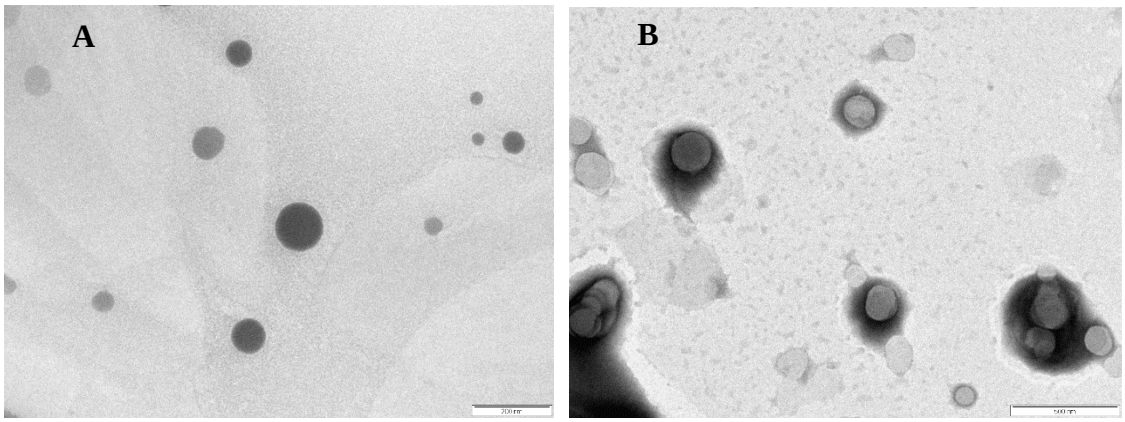

Figure S5. Surface morphology by TEM (A) LP-3 liposomes and (B) LP-CONH-RGD liposomes.

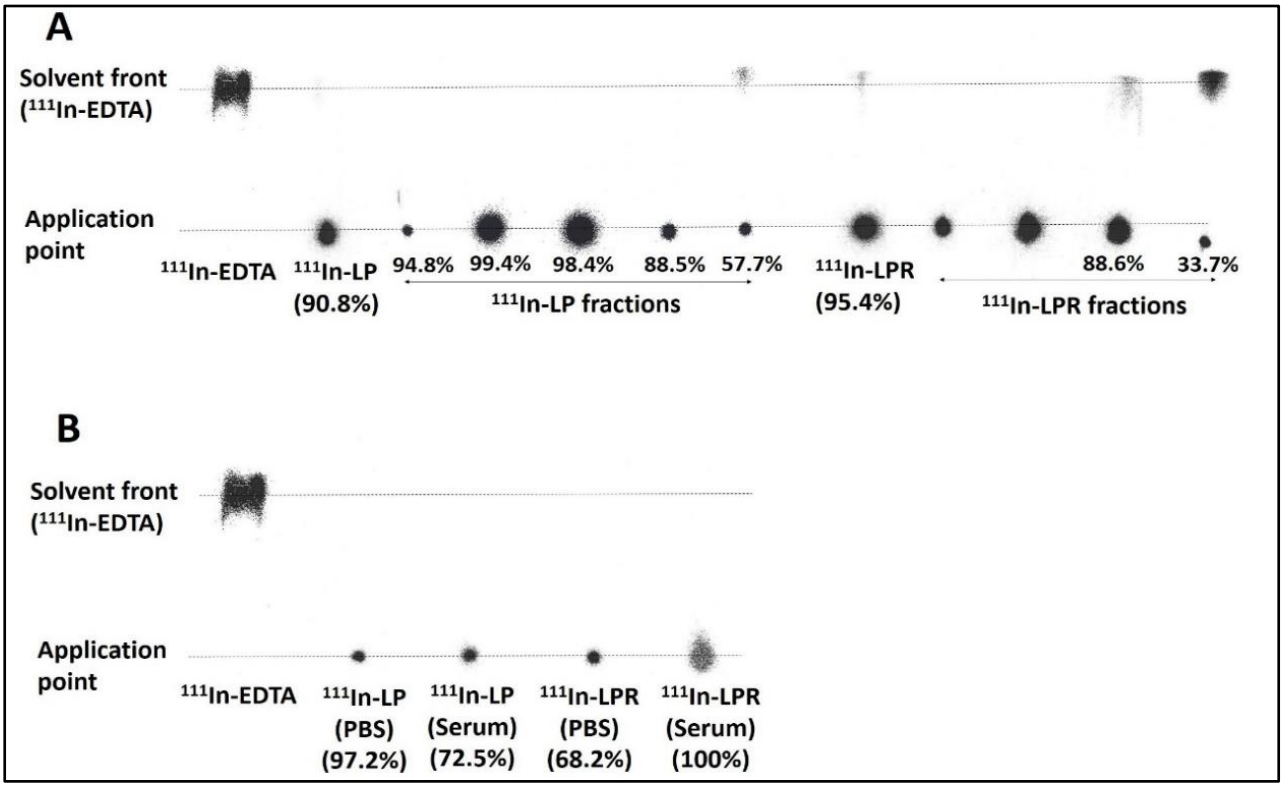

Figure S6. Radiolabelling efficiency of liposomes with indium (^{111}In) and radiolabelling stability in PBS and fetal bovine serum (FBS)
(A) TLC of the liposomes immediately after radiolabelling and TLC of column fractions of radiolabelled liposomes. (B) TLC of purified radiolabelled liposomes after incubation with both PBS and FBS for 24 h at 37 °C.

Table S1. Composition and formulation optimization results of ASPM liposomes

Batches	TL (% w/v)	DSPC:CHOL	ST (min)	Amp (%)	Drug (% w/w)	PS (nm)	PDI	ZP (mV)	% EE
LP-1	1	1:0.5	10	60	0.005	131.5± 10.4	0.222± 0.093	-47.6 ± 1.3	47.0± 4.1
LP-2	1.5	1:0.5	10	60	0.005	100.0± 9.0	0.191± 0.027	-50.8 ± 3.1	51.0± 4.4
LP-3	2	1:0.5	10	60	0.005	97.7± 1.5	0.216± 0.068	-51.2 ± 3.9	52.2± 3.6
LP-4	2.5	1:0.5	10	60	0.005	119.1± 11.2	0.235± 0.105	-53.6 ± 2.8	43.0± 3.3
LP-5	3	1:0.5	10	60	0.005	139.3± 9.3	0.284± 0.120	-55.1 ± 3.7	42.5± 3.8
LP-6	2	1:0.25	10	60	0.005	85.78± 1.8	0.244± 0.057	-50.8 ± 4.3	25.6± 2.4
LP-7	2	1:1	10	60	0.005	143.30 ± 12.21	0.267± 0.110	-54.4 ± 5.5	54.5± 5.0
LP-8	2	1:0.5	10	60	0.0025	80.43± 9.6	0.211± 0.053	-50.0 ± 2.7	39.9± 4.2
LP-9	2	1:0.5	10	60	0.0075	106± 12.8	0.105± 0.035	-41.5 ± 4.8	46.1± 5.8
LP-10	2	1:0.5	5	60	0.005	103.7± 9.8	0.224± 0.069	-49.3 ± 4.9	48.8± 2.9
LP-11	2	1:0.5	15	60	0.005	85.1± 9.2	0.189± 0.037	-51.1 ± 5.8	38.0± 3.2
LP-12	2	1:0.5	5	40	0.005	105.0± 8.4	0.245± 0.074	-48.1 ± 4.7	45.9± 4.3
LP-13	2	1:0.5	15	80	0.005	115.7± 8.8	0.294± 0.046	-48.4 ± 4.6	33.6± 3.1

Volume of dispersion: 10 mL; DSPC= 1,2-Distearoyl-sn-glycero-3-phosphocholine; CHOL= Cholesterol; ST= Sonication time; Amp= Sonication amplitude; PS= Particle size; PDI= Polydispersity index; ZP= Zeta Potential; EE= Entrapment efficiency.

Table S2. Composition of conjugated liposomes

Liposomes		DSPC: CHOL	Linker (mM)	RGD (mM)	Drug (0.005% ww)	Label
Plain liposomes	LP	1:0.5	−		✓	−
	LP-DiI	1:0.5	−	−	−	DiI: 0.5% w/w
-COOH functionalized liposomes	LP-COOH	1:0.5	0.2 (DSPE-PEG-COOH)	−	✓	−
	LP-CONH-RGD	1:0.5	0.2 (DSPE-PEG-COOH)	0.4	✓	−
Maleimide functionalized liposomes	LP-MAL	1:0.5	0.2 (DSPE-PEG-MAL)	−	−	−
	LP-MAL-RGD	1:0.5	0.2 (DSPE-PEG-MAL)	0.4	−	−
	LP-DTPA	1:0.5	−	−	−	RL (DTPA: 1% w/w)
	LP-MAL-RGD-DTPA	1:0.5	0.2 (DSPE-PEG-MAL)	0.4	−	RL (DTPA: 1% w/w)
	LP-MAL-RGD-DiI	1:0.5	0.2 (DSPE-PEG-MAL)	0.4	−	DiI: 0.5% w/w

DSPC= 1,2-Distearoyl-sn-glycero-3-phosphocholine; CHOL= Cholesterol

Table S3. The cell viability and permeability results of plain drug, LP-3 liposomes and LP-CONH-RGD

Cell line	ASPM conc. (μM/mL)	Plain drug	LP-3	LP-CONH-RGD
% Cell Viability				
Caco2 monoculture	1	99.6±6.8	97.3±5.9	97.5±6.1
	5	98.2±7.8	96.6±4.5	94.9±8.2
	10	99.1±6.3	91.8±6.2	96.0±6.3
	20	97.7±8.0	92.7±4.4	90.2±4.9
Caco2+RajiB co-culture	1	95.4±7.9	95.7±8.1	94.1±5.3
	5	92.1±4.9	91.8±6.8	91.3±7.2
	10	91.9±7.9	94.8±6.6	93.7±6.0
	20	91.9±5.8	91.8±6.4	92.7±7.8
Apparent permeability coefficient (Papp ($x10^{-6}$))				
Caco2 monoculture		4.1±0.3	26.2±1.8#	29.0±2.8#
Caco2+RajiB co-culture		5.0±0.2	34.5±1.7#	44.2±2.4#*

Significantly different ($p<0.05$) compared to corresponding values of plain drug
* Significantly different ($p<0.05$) compared to corresponding value of LP-3

References:

Martins, S., Tho, I., Souto, E., Ferreira, D., Brandl, M., 2012. Multivariate design for the evaluation of lipid and surfactant composition effect for optimisation of lipid nanoparticles. Eur. J. Pharm. Sci. 45, 613-623.

Shete, H., Patravale, V., 2013. Long chain lipid based tamoxifen NLC. Part I: Preformulation studies, formulation development and physicochemical characterization. Int. J. Pharm. 454, 573-583.

Sugita, P., Ambarsari, L., Farichah, F., 2013. Increasing amount and entrapment efficiency of chitosan-ketoprofen nanoparticle using utrasonication method with varied time and amplitude. IJRRAS 14, 612-618.

Victoria, M.M., David, C.J., 2003. Thermal and rheological study of lipophilic ethosuximide suppositories. Eur. J. Pharm. Sci. 19, 123-128.